

On the significance of the pitching axis location for Flapping Wing Systems of swept outlines under Spring Loaded or Active Control of the pitching motion.

Tsarsitalidis Vasileios¹, Politis Gerasimos²

¹ Post-Doctoral Researcher, School of Naval Architecture and Marine Engineering, National Technical University of Athens

² Professor, School of Naval Architecture and Marine Engineering, National Technical University of Athens

ABSTRACT

Emissions rules but also economy, demand ever higher efficiency but not at the expense of safety and comfort onboard a vessel. The area of biomimetics has been sought after in the past showing promising potential, but was abandoned, as the 70's energy crisis receded and technical issues made it unprofitable to pursue. Nowadays, the interest is being reheated, as experimental data and simulations promise high efficiencies, outstanding maneuverability and seakeeping qualities, while technical obstacles are being overcome. The problem of a spring loaded and/or controlled pitching motion of the wing is the natural sequel to the fully prescribed motions if a compromise of propulsive power and reduction of ship motions is the objective function for propulsor design, for the ship operating in a wavy environment.

In this paper, the effects of pitching axis position according to wing shape are explored by systematically employing the 3D boundary element solver with free wake UBEM (Politis 2011), coupled with a data generation code capable of handling the complex motions resulting for the case of a spring loaded and/or actively pitched wing. (Tsarsitalidis & Politis 2015). Geometrical and motion parameters are varied, with the aim of providing information vital for the design of such devices, such as power requirement, exerted forces and stability of the system, leading thus to estimating operational limitations.

Keywords

Biomimetics, Flapping foil propulsion; Spring loaded wing dynamics; Active pitch control; Boundary element method; Incompressible non-viscous unsteady lifting flows; Unsteady wake rollup.

1 INTRODUCTION

Biomimetic propulsors are becoming the subject of increasing interest, since they have proved to be of higher efficiency than conventional propellers, can employ a higher area of effect and have the potential for converting environmental (wave induced motions) energy to useful thrust. Recent research and development results concerning flapping foils and wings, have shown that such systems at optimum conditions could achieve significant thrust; see, e.g., Triantafyllou et al (2000, 2004), Taylor et al (2010), and in Politis & Tsarsitalidis (2014) a design method for such propulsors was proposed, while an inland waterway propulsor (O-Foil) has been successfully implemented in the Netherlands, and the concept of a wavepropulsor has been proven of high potential both numerically (Filippas & Belibassakis (2014) and Tsarsitalidis & Politis (2015)) and experimentally Bockmann & Steen (2014-2016). Additionally, the latest requirements and inter-governmental regulations related to vehicle technology for reduced pollution and environmental impact are becoming ever stricter, and response to the demand of greening of transport, while maintaining (if not increasing) the safety standards, has been recognized to be an important factor for the shipbuilding industry.

A main difference between a biomimetic propulsor and a conventional propeller is that the former absorbs its energy by two independent motions: the heaving motion and the pitching (wing) motion. For harmonically oscillating wings, the energy required for pitching has been proven to be orders of magnitude smaller than that for heaving, leading to the seek for pitch control strategies (Belibassakis & Politis (2013), Filippas, & Belibassakis (2014), Tsarsitalidis & Politis (2015)). In real sea conditions, the ship undergoes a moderate or higher-amplitude oscillatory motion due to waves, and the vertical ship motion could be exploited for providing one of the modes of combined/complex oscillatory motion of a biomimetic

propulsion system. At the same time, due to waves, wind and other reasons, ship propulsion energy demand in rough sea is increased well above the design condition, especially in the case of bow/quartering seas. An ideal biomimetic propulsor, would provide the required thrust efficiently, while absorbing energy from the wave induced motions (thus reducing them). The position of the pitching axis plays an important role on the dynamics of the system, affecting stability, power requirement and thrust production. Such effects are amplified and/or altered when swept and bio-inspired outlines are employed.

The modern history of biomimetics starts in 1935 with Gray's paradox, and theoretical developments start with the works of Sir James Lighthill (1969), T.Y. Wu (1971). A thorough review of those theories can be found in Sparenberg (2002). Extensive reviews of computational and experimental work in biomimetics can be found in the papers of Shyy (2010) regarding aerodynamics and aeroelasticity; of M. Triantafyllou (1991, 2004) regarding experimental developments and of Rozhdestvensky (2003) regarding all types of applications, even full scale, with additional care given to the work done by eastern scientists (i.e. Russians and Japanese). Interesting information is also included in the books by: (Shyy, Aono et al. 2010) and Taylor et al. (2011). Marine biomimetic propulsors are also discussed in the book of Bose (2010).

The scope of the present work is to initialize the investigation of the effects of shape and pitch axis in the behavior of flapping wing propulsors and give a frame of reference to the future designer and/or experimenter, who will need to decide upon the size/capacity of the mechanism which will be realized in an actual propulsor. To this end the unsteady boundary element code with free wake UBEM (Politis 2011), coupled with a 1-DOF hydro-elastic model of a spring driven wing, and the APC (Adaptive Pitch Control) algorithm as they have been introduced in Tsarsitalidis & Politis (2015), is systematically applied for a range of motion parameters, while varying the position of pitching axis for straight and swept wings of the same section and aspect ratio. Presented results indicate that biomimetic wings with either APC or spring loaded can have substantial abilities as ship propulsors and energy saving devices.

2 FORMULATION

2.1. Wing geometry, motion and panel generation.

For the general case of a flapping wing configuration, the independent variables which define the state of the system can be decomposed in two groups. The 'geometric' variables and the 'motion related' variables. For the selection of wing geometry the flapping wing series described in (Politis and Tsarsitalidis 2014) has been used. More specifically we have chosen a wing with $s/c=4$ where s denotes span and c the chord length. The outline and meshing of the wings used is

presented in Figure 1. A NACA0012 profile throughout the span is used for all cases. Finally to the geometric variables we have to add the pitching axis position. This is the subject of section 2.4.

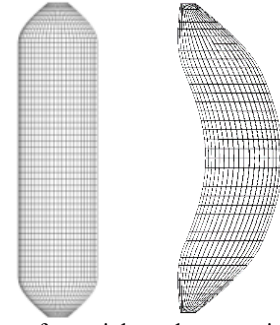


Figure 1 Geometry of a straight and swept wing of $s/c=4.0$

Regarding description of wing motion, for the cases considered in this paper, they can be decomposed in a translational part with velocity of advance U , a heaving part with instantaneous heaving amplitude $h(t)$ and a pitching motion with instantaneous pitch angle $\theta(t)$. For the simplest 'prescribed motion' case, heaving and pitching can be independently selected harmonic (sinusoidal) functions of frequency f with amplitudes h_0, θ_0 and some phase angle ψ between them (in the current paper $\psi = 90^\circ$). For the most advanced cases considered in this work, i.e. the spring loaded and the actively pitched wing, the pitching motion is dependent from the heaving motion in general in a complex way. More specifically for the spring loaded case instantaneous pitch results from the equilibrium of moments, equation (4), and the properties of the spring/damper system (elastic constant K and damping factor C) acting as parameters for the calculation of instantaneous pitch. For the actively pitched wing, instantaneous pitch is selected as a function of the time rate of heave and the velocity of advance (Politis&Politis 2014).

With the motion parameters known, the instantaneous angle of attack $a(t)$ of each wing (wing is assumed untwisted) with respect to the undisturbed flow is given by:

$$a(t) = \theta(t) - \tan^{-1} \left(\frac{dh(t)/dt}{U} \right) \quad (1)$$

Additionally, as in previous works, Str denotes the Strouhal number defined by:

$$Str = \frac{f \cdot h}{U}, h = 2h_0 \quad (2)$$

where h denotes the heave height. Finally the Thrust coefficient is defined by:

$$C_T = \frac{T}{0.5\rho U^2 S} \quad (3)$$

where T is the calculated mean thrust and S the swept area covered by the wing in motion, given by $S = s \cdot 2h$.

2.2 Spring loaded wing simulations

Assuming a foil of chord (c) as in Figure 2, the pitching axis (pa), the center of pressure (cp) and the center of mass (cm) are critical points for the stability of the system. From flight mechanics it is known that having the pitching axis ahead of the pressure center and having the pressure center ahead of the center of mass, produces an inherently stable system.

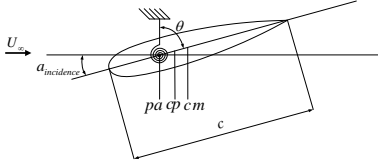


Figure 2 Schematic of Spring Loaded wing system.

In order to find the pitching angle at each time t , the following differential equation has to be solved for $\theta(t)$:

$$M_{ext}(t) = I\ddot{\theta}(t) + C\dot{\theta}(t) + K\theta(t) \quad (4)$$

where M_{ext} is the external moment (in the specific case, the hydrodynamic moment), I the moment of inertia about pitch axis, C the damping factor and K the spring stiffness.

The solution of the coupled problem is done in an explicit scheme, where the hydrodynamic moment $M_{ext}(t)$ calculated at each step is used in order to find the pitch angle for the next time step. As long as the time step is small enough and pitch angle variations are also small, this scheme is expected to be robust and accurate, as long as time integrations (solution of (4) for constant $M_{ext}(t)$ and given time step) are made with care. For the time integration of (4) a Newmark $-\beta$ scheme is applied. (Chopra 2007).

Regarding wing geometry and properties we have worked as follows: For the wing, the geometry is selected as discussed in section 2.1 (figure 1, $s/c=4.0$) and a uniform mass distribution, with density that of solid material of neutral buoyancy and the same shape, was assumed. Then, the mass, center of mass and moment of inertia can be calculated by employing a CAD software using either numerical integrations or empirical rules (found in textbooks)

Regarding selection of the damping the definition for 'damping ratio' is taken from the dynamics of harmonic oscillators:

$$\zeta = \frac{C}{2\sqrt{IK}} \quad (5)$$

The value $\zeta=1$ was chosen for the initial explorations, as it is desirable that the system is not allowed to resonate with the excitation, but also that it does not delay to respond. Thus damping factor C becomes a function of K , and the differential equation (4) depends solely on K and the inertia properties of the wing system.

2.3 Active Pitch Control

Active pitch control as introduced in Politis and Politis (2014) was taken as a starting point and developed further by Tsarsitalidis & Politis (2015). In the current paper the Adaptive Pitch Control (APC) algorithm is employed, as introduced by the latter. More specifically, from the original of (Politis and Politis 2014), the pitch angle at each time step is defined as:

$$\theta(t) = w \tan^{-1}((dh/dt)/U) \quad (6)$$

where w is a control parameter ranging from zero to one that is set beforehand. Knowing the expected heave amplitude, frequency and speed of advance, and knowing that:

$$a(t) = (1-w) \tan^{-1}((dh/dt)/U) \quad (7)$$

the parameter w can be set to a number that the maximum angle of attack does not exceed a defined value.

The constant parameter w is substituted with a variable $w(t)$ and keeping in mind the objective of keeping the angle of attack below a given value, a new law for $w(t)$ is obtained by finding the lowest $w(t)$ satisfying the inequality:

$$A \geq (1-w(t)) \tan^{-1}(dh/dt/U), A = A_{max} \quad (8)$$

The value found, is then substituted in (6), to give the pitching angle. This gives at a minimal addition of computational cost, a different, non-harmonic profile of pitching motion, where the angle of attack is kept below the given value A_{max} , but also equal to it for a longer part of the motion. In Figure 3, a time series of heaving position (Heave), pitch angle (rot), resulting angle of attack (local_attack), $w(t)$ (ww) and Thrust produced (fx, negative is for forward thrust) are presented for an indicative case of foil of $s/c=4$ at $Str=0.4$ and Target $A_{max}=17^\circ$.

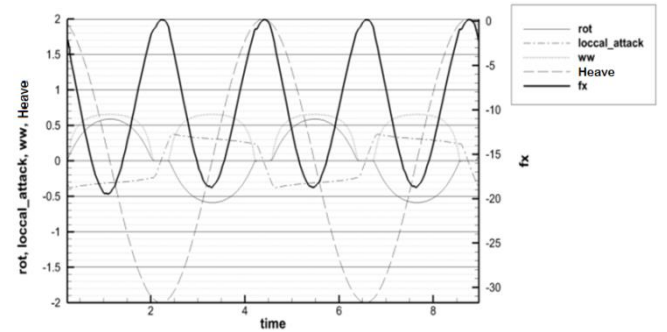


Figure 3 Time series of simulation of an APC foil of $s/c=4$ at $Str=0.4$ and Target $A_{max}=17^\circ$.

2.4 Range of Pitching Axis Position

For the selection of the pitching axis position the selection that was made in Tsarsitalidis & Politis (2015) is reconsidered and investigated. The requirement of stable motion patterns leads to select it in front of the center of

pressures. From linear, steady 2D wing theory it is known that the center of pressures coincides with the one quarter chord point from the leading edge and in the aforementioned paper had shown that this is the case for the problem in hand as well and carried on with positioning the pitching axis at that point. For this investigation the pitching axis was systematically varied from the leading edge to 0.2c. Obviously, the change in moment of inertia is taken into account in the dynamics of the system.

3 RESULTS AND DISCUSSION

3.1 Spring Loaded Wing Systematic Simulations

Systematic simulations were made for Str ranging from 0.1 to 0.7 and K/ρ from 5 to 21 (ρ denotes the fluid density in kg/m^3). The calculated thrust coefficient C_T against K/ρ is shown in Figs. 2-7 in a parametric form with parameters the Strouhal number (thicker lines) and the efficiency (thinner lines). The C_T against pitch angle ‘theta’ chart, with the same parametric lines, produced for the same wings under fully prescribed motion (with phase angle between heave and pitch equal to 90deg), is given in Figures 8 and 9 for comparison. Notice that for the spring loaded case, C is calculated by enforcing $\zeta=1$. Thus the only free parameter in equation (4) for the determination of time dependent pitch $\theta(t)$ is K . Thus K is the ‘proper replacement’ for ‘theta’ in C_T plots for the case of a spring loaded wing. Figures 2-4 show the plots for straight wing and varying pitching axis position and 5-7 show the same for swept wings. It is observed that the spring loaded wing produces substantial thrust, but the maximum efficiency is smaller and for a narrower area of parameters compared to a prescribed motion wing. However, there is a clear trend showing that moving the pitching axis further to the front gives better efficiency at the cost of thrust coefficient. Especially for the case of swept wings, the efficiency is significantly increased, giving a maximum of 0.725, very close to the 0.74 for prescribed, pointing to the possibility of further increase with moving the pitching axis further forward, but also making tests with underdamped conditions. It should be noted that swept wings, but also straight with axis far ahead of the hydrodynamic center, appear to be very stable, thus the requirement for $\zeta=1$ can be relaxed. When the spring loaded wing is used as an energy saving device (i.e. heaving energy is taken from ship motions reducing them) the efficiency of the system looks irrelevant, as the useful propulsive power divided by the mechanical power given, becomes infinite. Notice that even in this case the conventional efficiency contained in figures 2-7 characterize how efficiently the spring loaded wing transforms heaving motions to thrust and thus the problem of efficiency optimization of the spring properties in connection with the solution of the coupled wing-ship problem (e.g.

Belibasakis&Politis 2013) is the correct design setup for a spring loaded wing propulsor. Closing this section it should be noted the existing knowledge, that spring loaded wings operate well only in limited conditions, has to be reassessed, especially for swept wings.

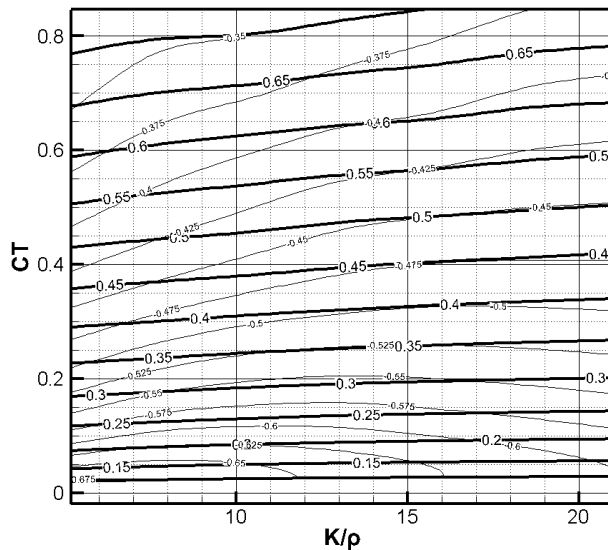


Figure 4 $C_T - K/\rho$ chart for a straight wing $s/c=4$, $h/c=1.5$, with pitch axis at L.E.. Thicker lines are for Strouhal number and thinner, are for efficiency.

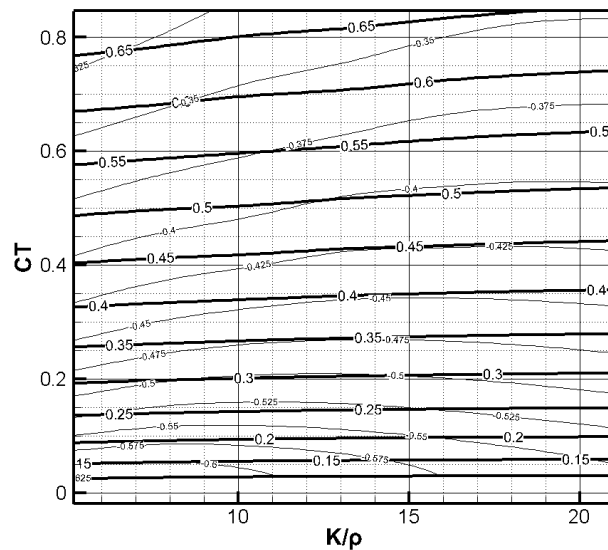


Figure 5 $C_T - K/\rho$ chart for a straight wing $s/c=4$, $h/c=1.5$, with pitch axis at 0.1c from L.E.. Thicker lines are for Strouhal number and thinner, are for efficiency.

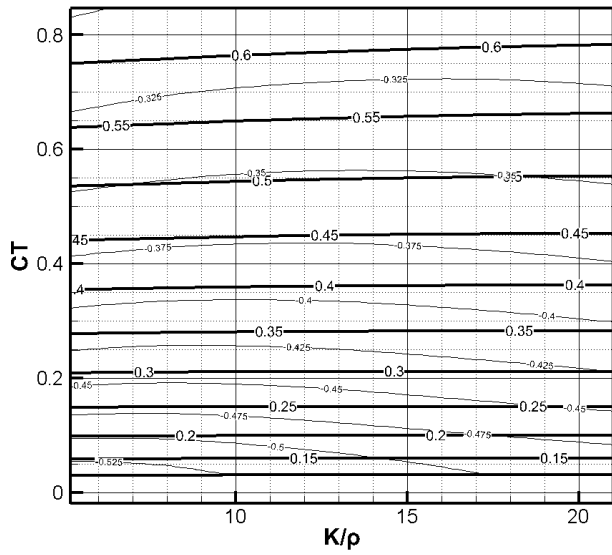


Figure 6 $C_T - K / \rho$ chart for a straight wing $s/c=4$, $h/c=1.5$, with pitch axis at $0.2c$ from L.E.. Thicker lines are for Strouhal number and thinner, are for efficiency.

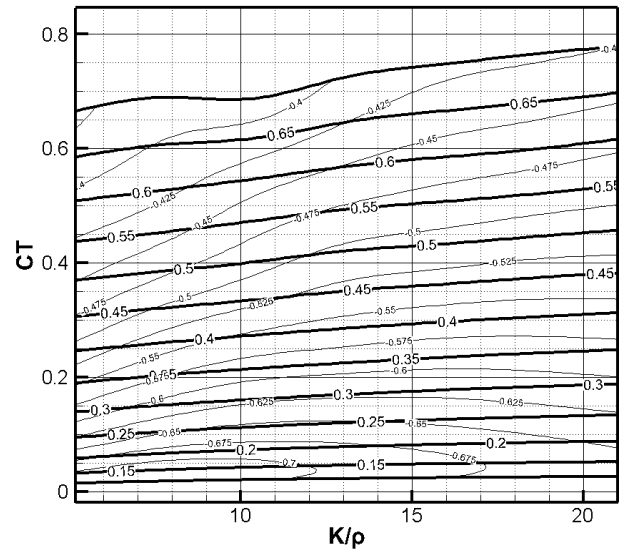


Figure 8 $C_T - K / \rho$ chart for a swept wing $s/c=4$, $h/c=1.5$, with pitch axis at $0.1c$ from L.E.. Thicker lines are for Strouhal number and thinner, are for efficiency.

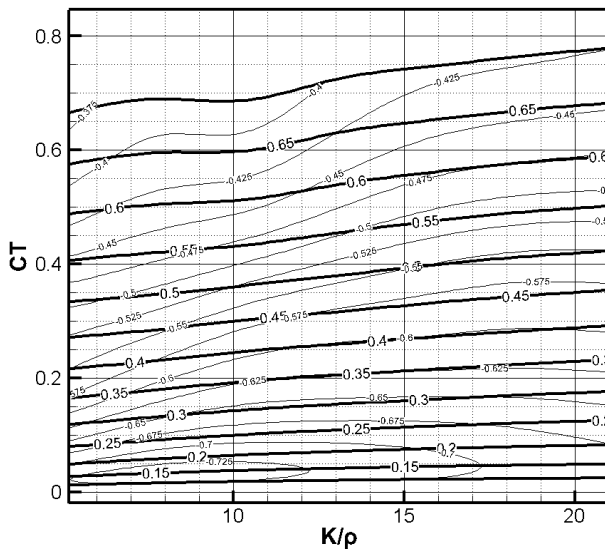


Figure 7 $C_T - K / \rho$ chart for a swept wing $s/c=4$, $h/c=1.5$, with pitch axis at L.E.. Thicker lines are for Strouhal number and thinner, are for efficiency.

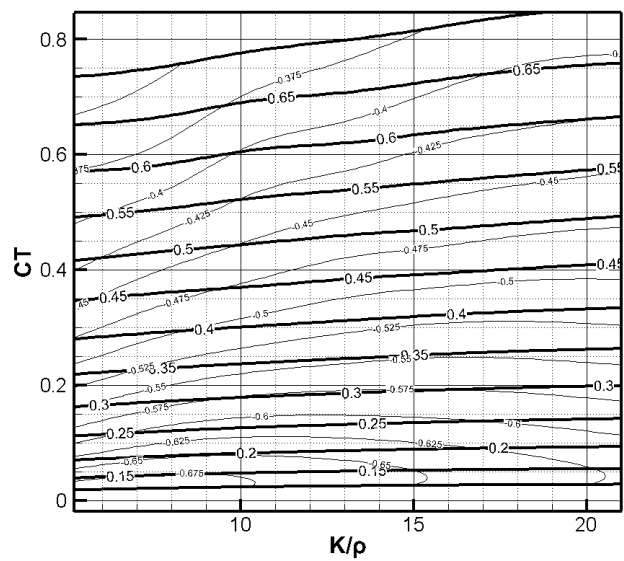


Figure 9 $C_T - K / \rho$ chart for a swept wing $s/c=4$, $h/c=1.5$, with pitch axis at $0.2c$ from L.E.. Thicker lines are for Strouhal number and thinner, are for efficiency.

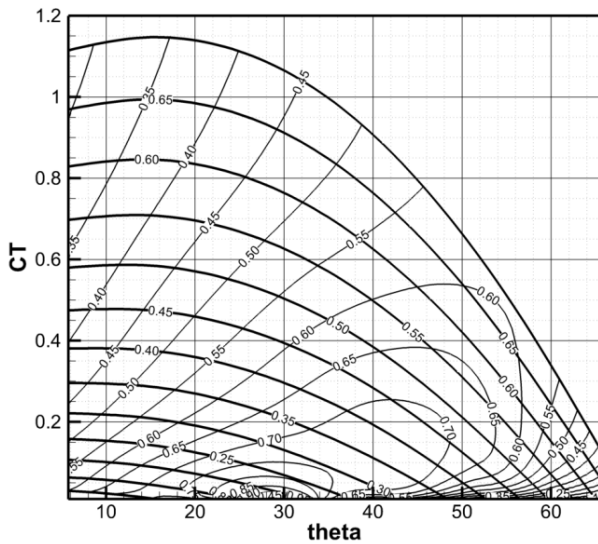


Figure 10 $C_T - \theta_0$ chart for a straight wing of $s/c=4$, $h/c=1.5$.

Thin contour lines are for Efficiency and thick ones are for Strouhal Number, theta denotes the pitch angle in degrees (from Politis & Tsarsitalidis (2014))

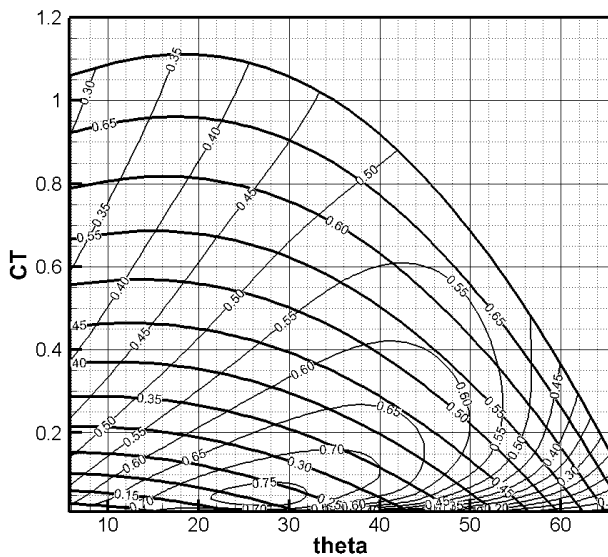


Figure 11 $C_T - \theta_0$ chart for the swept wing of $s/c=4$, $h/c=1.5$.

Thin contour lines are for Efficiency and thick ones are for Strouhal Number, theta denotes the pitch angle in degrees

3.2 Active Pitch Control Systematic Simulations

The APC relation (8) has been applied for a harmonically heaved wing for a range of Strouhal numbers and maximum angles of attack A_{max} as visible in the systematic $C_T - A_{max}$ diagrams of figures 10-15. In all cases, high efficiency and thrust coefficient is observed for a broad region of A_{max} , indicating that the system is very promising for a propulsor, even at steady cases. The high efficiency at high thrust

coefficients shows that the system is also advantageous in high load conditions. Variation of the pitching axis shows different behavior than the spring loaded, as having the pitch axis moving towards the hydrodynamic center, gives improved performance. It is also noticeable, that thrust coefficients (for the same combination of Str, Target A_{max}) are very similar for each set of simulations, showing that the position of the pitching axis affects the power requirement more than the thrust produced. Concluding, an actively pitch controlled wing seems a very good selection if both propulsive efficiency and energy extraction from ship motions is the design target.

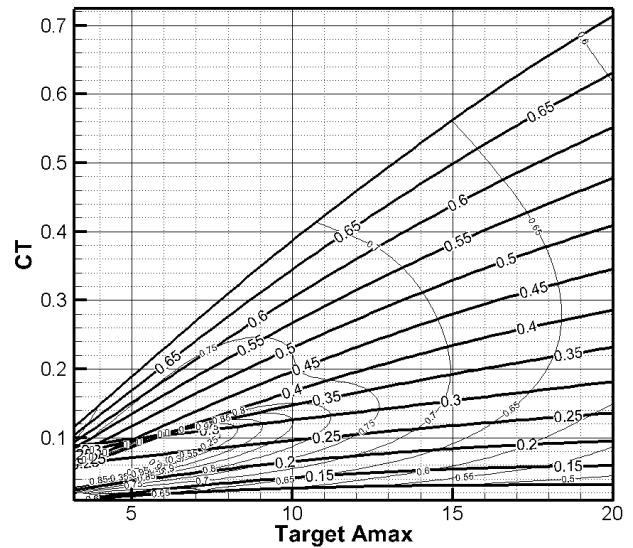


Figure 12 $C_T - A_{max}$ chart for a straight wing $s/c=4$, $h_0/c=1.5$, Pitching axis at L.E., under simple harmonic heaving motion and APC. Thicker lines are for Strouhal number and thinner, are for efficiency.

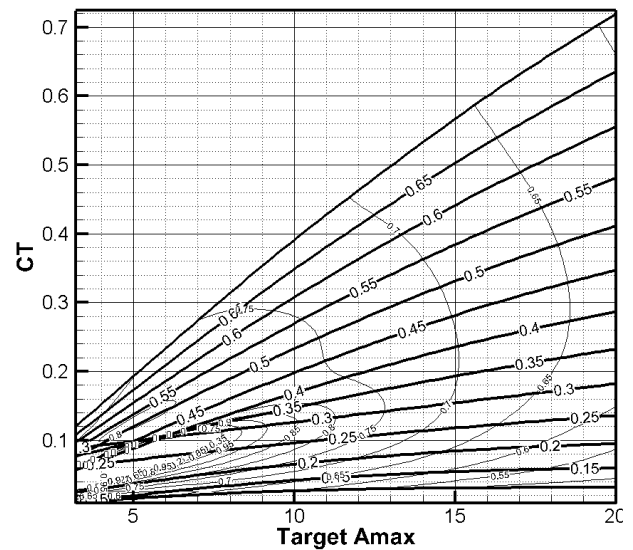


Figure 13 $C_T - A_{max}$ chart for a straight wing $s/c=4$, $h_0/c=1.5$, Pitching axis at $0.1c$ from L.E., under simple harmonic heaving motion and APC. Thicker lines are for Strouhal number and thinner, are for efficiency.

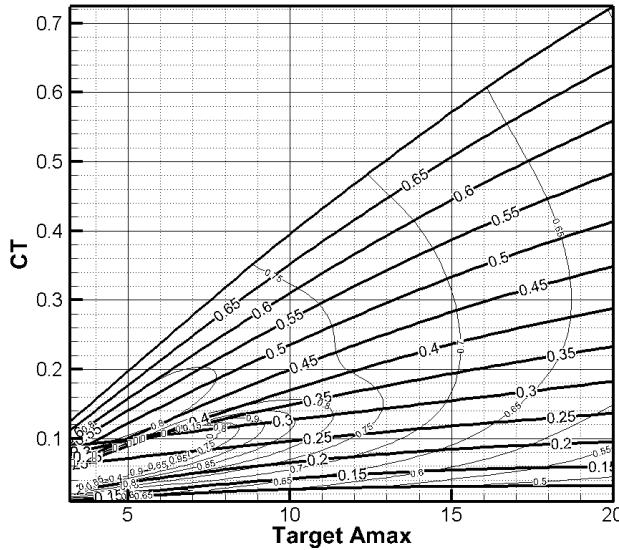


Figure 14 $C_T - A_{max}$ chart for a straight wing $s/c=4$, $h_0/c=1.5$, Pitching axis at $0.2c$ from L.E., under simple harmonic heaving motion and APC. Thicker lines are for Strouhal number and thinner, are for efficiency.

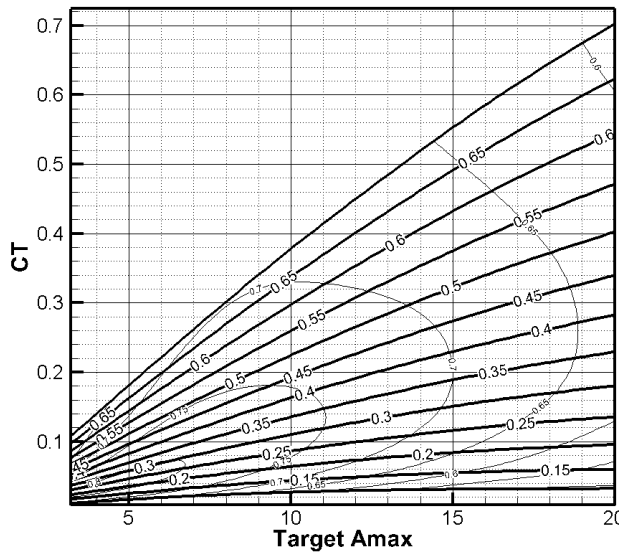


Figure 15 $C_T - A_{max}$ chart for a swept wing $s/c=4$, $h_0/c=1.5$, Pitching axis at L.E., under simple harmonic heaving motion and APC. Thicker lines are for Strouhal number and thinner, are for efficiency.

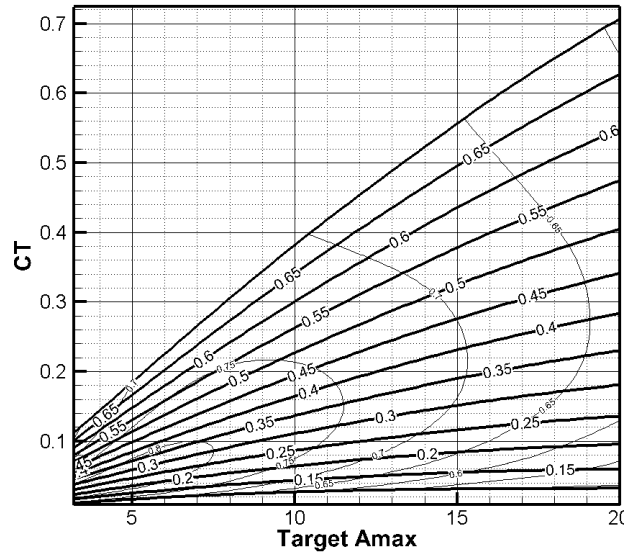


Figure 16 $C_T - A_{max}$ chart for a swept wing $s/c=4$, $h_0/c=1.5$, Pitching axis at $0.1c$ from L.E., under simple harmonic heaving motion and APC. Thicker lines are for Strouhal number and thinner, are for efficiency.

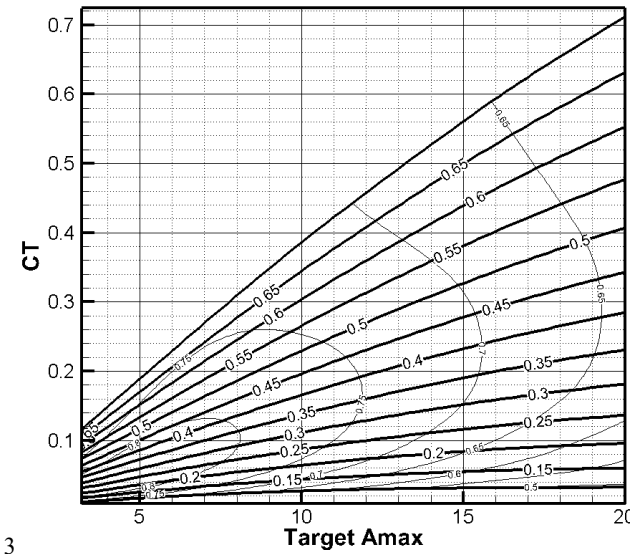


Figure 17 $C_T - A_{max}$ chart for a swept wing $s/c=4$, $h_0/c=1.5$, Pitching axis at $0.2c$ from L.E., under simple harmonic heaving motion and APC. Thicker lines are for Strouhal number and thinner, are for efficiency.

4 CONCLUSIONS AND FUTURE WORK

An initial exploration of the effects of pitching axis position on wings with passive (spring loaded) and active pitch control has been presented. Both systems seem promising, with the passively controlled wings showing improved behavior as the axis moves ahead and even better improvement for swept wings. The actively controlled wings

are affected differently, as moving the axis forward increases the power requirement, having secondary effects on the developed thrust. In all cases of APC, higher efficiencies are observed for high load conditions (i.e. higher Strouhal numbers and/or smaller swept area), indicating good applicability for cases of very restricted propulsor size (i.e. shallow waters/ small stern) and low speed-high thrust applications making it an attractive pitch profile strategy, even for calm water conditions, aside of the good adaptability in complex environmental conditions. On the other hand, the spring loaded wings, being independent of electronics and the need to determine the incoming flow, are promising for custom-made design in cases of one design point ship operation. To give the reader a frame of reference in Politis & Tsarsitalidis (2014) it was shown that for the design condition of most large ships the required Thrust Coefficient would be of the order of 0.12 to 0.15, which would correspond to Strouhal numbers of the range of 0.25 to 0.35. Further investigation has to be made for both cases. For the case of spring loaded wings, further variation of the effect of skew is to be explored, while also investigating the effect the damping factor is also important, as the stability issues seem to be minimal when the pitching axis is close to the L.E. Different methods of control are also to be investigated, such as more sophisticated systems that would use the data from extensive simulations for system recognition that would lead to the creation of a state-space controller for thrust production in random motions (Wen et.al 2010). Ultimate goal would be to simulate (numerically and experimentally) the coupled problem of the self-propelled vessel, where interaction factors would be determined and all aspects of propulsor design would be complete.

REFERENCES

- Belibassakis, K. A. and G. K. Politis (2013). "Hydrodynamic performance of flapping wings for augmenting ship propulsion in waves." Ocean Engineering 72: 227-240.
- Belibassakis K.A., Filippas, E., (2015). "Ship propulsion in waves by actively controlled flapping foils", Applied Ocean Research 52, 1-11
- Bøckmann, E. and S. Steen (2014). "Experiments with actively pitch-controlled and spring-loaded oscillating foils." Applied Ocean Research 48: 227-235.
- Bøckmann, E. and S. Steen (2016). "Model test and simulation of a ship with wavefoils". Applied Ocean Research 57: 8-18
- Chopra, A. K. (2007). Structural Dynamics
- Filippas, E., Belibassakis K.A. (2014) "Hydrodynamic analysis of flapping-foil thrusters operating beneath the free surface and in waves", Engineering Analysis with Boundary Elements, Vol.41, 47-59.
- Politis, G. and K. Politis (2014). "Biomimetic propulsion under random heaving conditions, using active pitch control." Journal of Fluids and Structures 47: 139-149.
- Politis, G. K. (2011). "Application of a BEM time stepping algorithm in understanding complex unsteady propulsion hydrodynamic phenomena." Ocean Engineering 38(4): 699-711.
- Politis, G. K. and V. T. Tsarsitalidis (2014). "Flapping wing propulsor design: An approach based on systematic 3D-BEM simulations." Ocean Engineering 84: 98-123.
- Rozhdestvensky, K. V. and V. A. Ryzhov (2003). "Aerohydrodynamics of flapping-wing propulsors." Progress in Aerospace Sciences 39(8): 585-633.
- Shyy, W., H. Aono, S. K. Chimakurthi, P. Trizila, C. K. Kang, C. E. S. Cesnik and H. Liu (2010). "Recent progress in flapping wing aerodynamics and aeroelasticity." Progress in Aerospace Sciences 46(7): 284-327.
- Sparenberg, J. A. (2002). "Survey of the mathematical theory of fish locomotion." Journal of Engineering Mathematics 44(4): 395-448.
- Triantafyllou, M. S., A. H. Techet and F. S. Hover (2004). "Review of experimental work in biomimetic foils." IEEE Journal of Oceanic Engineering 29(3): 585-594.
- Triantafyllou, M. S., G. S. Triantafyllou and R. Gopalkrishnan (1991). "Wake mechanics for thrust generation in oscillating foils." Physics of Fluids A 3(12): 2835-2837.
- Tsarsitalidis V.T., Politis (2015), "Simulating Biomimetic Propulsors under spring loading and/or active control for the pitching motion of the wings", Fourth International Symposium on Marine Propulsors SMP'15, Austin, Texas, USA.
- Wen, L., Z. Fan, T. Wang and J. Liang (2010). "Fuzzy control of biomimetic propulsion using flapping foil." Iqiren/Robot 32(3): 306-313.
- Wu, T. Y. (1971). "Hydromechanics of swimming propulsion. Part 1. Swimming of a two-dimensional flexible plate at variable forward speeds in an inviscid fluid." J. of Fluid Mechanics 46: 337-355.
- Zhu, Q. (2011). "Optimal frequency for flow energy harvesting of a flapping foil." Journal of Fluid Mechanics 675: 495-517.